Electronic Supplementary Material (ESI) for Chemical Communications.

Supporting Information

Synthesis of homometallic divalent lanthanide organoimides from benzyl complexes

Benjamin M. Wolf, Christoph Stuhl, and Reiner Anwander*

Institut für Anorganische Chemie, Eberhard Karls Universität Tübingen, Auf der Morgenstelle 18, 72076 Tübingen, Germany

*E-mail for R.A.: reiner.anwander@uni-tuebingen.de.

Table of Contents

Experimental Section

General Considerations. All manipulations were performed under rigorous exclusion of air and moisture, using standard Schlenk, high-vacuum, and glovebox techniques (MB Braun MB200B; <1 ppm O_2, <1 ppm H_2O, argon atmosphere). The solvents toluene and tetrahydrofuran (thf) were purified using Grubbs columns (MBraun SPS, solvent purification system). Tetrahydrofuran was stored over freshly activated molecular sieves (3 Å). Tetrahydropyran (thp, 98+%, Alfa Aesar) and [D_8]thf (99.5%, Euriso-top) were dried by distillation from Na/K-alloy. 1,2-Dimethoxyethane (dme, 99%, ABCR) and 2,6-diisopropylaniline (H_2NDipp, 97%, Sigma-Aldrich) were dried by distillation from CaH_2. All solvents were stored inside a glovebox. Iodides $LnI_2(thf)_2$,[1] benzylpotassium $[K(CH_2Ph)]_n$,[2] and triphenylsilylamine (H_2NSiPh_3)[3] were synthesised according to literature procedures. The NMR spectra of air and moisture sensitive compounds were recorded by using *J. Young* valve NMR tubes on a *Bruker AVII+400* (^{1}H: 400.13 MHz; ^{13}C: 100.61 MHz) spectrometer. ^{1}H and ^{13}C NMR chemical shifts are referenced to solvent residual resonances and reported in *parts per million*, relative to tetramethylsilane (TMS). Coupling constants are given in Hertz. IR spectra were recorded on a *NICOLET 6700 FTIR* spectrometer with a DRIFT cell (KBr window), and the samples were prepared in a glovebox and mixed with KBr powder. Elemental analyses were performed on an *Elementar Vario Micro Cube*. All reactions were performed with glass-coated magnetic stirring bars.

$[Yb(CH_2Ph)_2]_n$ (1-Yb). To a pre-cooled solution (–30 °C) of $[YbI_2(thf)_2]$ (600 mg, 1.05 mmol) in thf (15 mL) a pre-cooled solution (–30 °C) of $[K(CH_2Ph)]_n$ (274 mg, 2.10 mmol) in thf (5 mL) was added. The color of the solution changed immediately from red to a dark orange and a white precipitate was formed. The reaction mixture was stirred at ambient temperature for 4 h and then the solvent was removed partially to about 5 mL. The white solid (KI) was removed by centrifugation and additionally washed with 2 mL of thf. To the combined thf solutions toluene (2 mL) was added and the nearly black solution was filtered. The solvents were removed under reduced pressure. Trituration of the dark brown oily residue

with toluene (15 mL) at ambient temperature for 2 h led to formation of a black solid which was isolated, washed with toluene (2x 5 mL) and dried at reduced pressure. Yield: 323 mg, 0.91 mmol, 87%. Although NMR data of the obtained product revealed no impurities, elemental analyses showed slight deviations, most likely due to traces of residual iodide which could not be separated in the workup procedure. An analytically very pure product could be obtained by crystallisation from thp (*vide infra*) and subsequent removal of coordinated donor solvent at reduced pressure. ^{1}H NMR (400 MHz, [D$_8$]thf, 26 °C): δ 6.50 (m, 4H, *m*-Ar*H*), 6.32 (d, 4H, $^{3}J_{HH}$ 7.1 Hz, *o*-Ar*H*), 5.74 (t, 2H, $^{3}J_{HH}$ 6.8 Hz, *p*-Ar*H*), 1.58 (s, 4H, C*H*$_2$Ph) ppm. ^{13}C{^{1}H} NMR (101 MHz, [D$_8$]thf, 26 °C): δ 160.0 (*ipso*-ArC), 128.6 (*m*-Ar*C*), 119.4 (*o*-Ar*C*), 109.2 (*p*-Ar*C*), 48.1 (*C*H$_2$Ph) ppm. DRIFT ($\tilde{\nu}$): 3055 (w), 2999 (w), 2969 (w), 2621 (vw), 2592 (vw), 1919 (vw), 1796 (vw), 1580 (vs), 1542 (w), 1521 (w), 1477 (vs), 1326 (w), 1298 (m), 1276 (s), 1256 (m), 1173 (s), 1146 (w), 1089 (w), 1013 (w), 989 (w), 863 (w), 769 (s), 734 (s), 691 (s), 652 (m), 544 (m), 524 (m), 513 (m), 495 (m) cm^{-1}. Elemental analysis (%) calculated for $C_{14}H_{14}Yb$ (355.32 g/mol): C 47.32, H 3.97, N 0.00; found: C 46.60, H 3.93, N 0.30.

[(thp)$_4$Yb(CH$_2$Ph)$_2$] (1-Yb^{thp}). Solid [Yb(CH$_2$Ph)$_2$]$_n$ (**1-Yb**, 50 mg, 0.14 mmol) was dissolved in tetrahydropyran (thp, 1 mL). Storage of the solution at –35 °C for 2 weeks afforded the product as dark red crystals which readily lost coordinated donor solvent even at ambient pressure. The crystals therefore were separated from the mother liquor and dried at ambient temperature under an inert atmosphere of Ar. Crystallised yield: 59 mg, 0.08 mmol, 60%. These crystals were also suitable for an X-ray structure analysis. ^{1}H NMR (400 MHz, [D$_8$]thf, 26 °C): δ 6.50 (m, 4H, *m*-Ar*H*), 6.32 (d, 4H, $^{3}J_{HH}$ 7.6 Hz, *o*-Ar*H*), 5.75 (t, 2H, $^{3}J_{HH}$ 7.0 Hz, *p*-Ar*H*), 3.53 (m, 12H, OC*H*$_2$ thp), 1.60 (m, 6H, C*H*$_2$ thp), 1.58 (s, 4H, C*H*$_2$Ph), 1.50 (m, 12H, C*H*$_2$ thp) ppm. ^{13}C{^{1}H} NMR (101 MHz, [D$_8$]thf, 26 °C): δ 160.1 (*ipso*-Ar*C*), 128.7 (*m*-Ar*C*), 119.5 (*o*-Ar*C*), 109.3 (*p*-Ar*C*), 69.2 (O*C*H$_2$ thp), 48.1 (*C*H$_2$Ph), 27.8 (*C*H$_2$ thp), 24.7 (*C*H$_2$ thp) ppm. DRIFT ($\tilde{\nu}$): 3050 (w), 2944 (s), 2846 (w), 1573 (vs), 1518 (vw), 1475 (s), 1388 (vw), 1352 (vw), 1326 (w), 1274 (m), 1191 (w), 1172 (m), 1149 (w), 1090 (w), 1076 (w), 1032 (m), 984 (w), 966 (w), 863 (m), 802 (m), 745 (vs), 699 (vs), 679 (vs), 659 (vs), 649 (vs), 568 (m), 528 (s), 511 (s), 404 (w) cm^{-1}. Elemental analysis (%) calculated for $C_{34}H_{54}O_4Yb$ (699.86 g/mol): C 58.35, H 7.78, N 0.00; found: C 57.51, H 7.43, N 0.04.

[(dme)$_2$Yb(CH$_2$Ph)$_2$] (1-Yb^{dme}). Solid [Yb(CH$_2$Ph)$_2$]$_n$ (**1-Yb**, 60 mg, 0.17 mmol) was dissolved in 1,2-dimethoxyethane (dme, 0.5 mL) and 0.5 mL of toluene were added. The solution was immediately cooled to –35 °C which after storage for 5 days led to the formation

of deep red crystals. The crystals were separated from the mother liquor and dried at ambient temperature under an inert atmosphere of Ar. Crystallised yield: 47 mg, 0.09 mmol, 52%. These crystals were also suitable for X-ray structure analysis. ^{1}H NMR (400 MHz, [D$_8$]thf, 26 °C): δ 6.52 (m, 4H, *m*-Ar*H*), 6.34 (d, 4H, $^{3}J_{HH}$ 7.6 Hz, *o*-Ar*H*), 5.77 (t, 2H, $^{3}J_{HH}$ 7.0 Hz, *p*-Ar*H*), 3.43 (s, 8H, C*H*$_2$ dme), 3.28 (s, 12H, C*H*$_3$ dme), 1.58 (s, 4H, C*H*$_2$Ph) ppm. ^{13}C{^{1}H} NMR (101 MHz, [D$_8$]thf, 26 °C): δ 159.9 (*ipso*-Ar*C*), 128.7 (*m*-Ar*C*), 119.6 (*o*-Ar*C*), 109.4 (*p*-Ar*C*), 72.7 (*C*H$_2$ dme), 59.1 (*C*H$_3$ dme), 48.1 (*C*H$_2$Ph) ppm. DRIFT ($\tilde{\nu}$): 3048 (w), 2991 (m), 2935 (m), 2828 (w), 2579 (vw), 2266 (vw), 1922 (vw), 1782 (vw), 1680 (vw), 1580 (s), 1538 (w), 1480 (m), 1452 (m), 1366 (w), 1329 (w), 1290 (m), 1247 (s),1190 (w), 1172 (m), 1147 (w), 1108 (m), 1068 (vs), 1022 (m), 981 (m), 857 (s), 841 (m), 800 (m), 745 (s), 733 (s), 690 (vs), 653 (vs), 643 (vs), 631 (vs), 558 (m), 528 (s), 504 (vs) cm^{-1}. Elemental analysis (%) calculated for $C_{22}H_{34}O_4Yb$ (535.56 g/mol): C 49.34, H 6.40, N 0.00; found: C 48.88, H 6.18, N 0.03.

[Sm(CH$_2$Ph)$_2$]$_n$ (1-Sm). Following the procedure described for **1-Yb** using $SmI_2(thf)_2$ (401 mg, 0.73 mmol) dissolved in 5 mL of thf and [K(CH$_2$Ph)]$_n$ (191 mg, 1.46 mmol) dissolved in 3 mL of thf afforded **1-Sm** as a black solid (239 mg, 0.72 mmol, 98%). Elemental analyses showed considerable deviations, most likely due to traces of residual iodide which could not be separated in the workup procedure. DRIFT ($\tilde{\nu}$): 3052 (w), 2991 (w), 2877 (w), 2566 (vw), 1915 (vw), 1782 (vw), 1683 (vw), 1583 (vs), 1569 (vs), 1534 (w), 1478 (vs), 1444 (w), 1326 (w), 1283 (s), 1174 (s), 1148 (w), 1035 (w), 979 (m), 848 (w), 800 (vw), 741 (s), 701 (s), 665 (m), 651 (m), 536 (s), 512 (m), 484 (m) cm^{-1}. Elemental analysis (%) calculated for $C_{14}H_{14}Sm$ (332.63 g/mol): C 50.55, H 4.24, N 0.00; found: C 48.63, H 4.38, N 0.07.

[(do)$_3$Sm$_2$(CH$_2$Ph)$_4$] (1-Sm^{do}). A solution of **1-Sm** (50 mg) in thf/thp (2 mL; 1:2) was carefully layered with *n*-hexane (1 mL) and stored at –35 °C for one week which led to the formation of almost black crystals which were suitable for X-ray structure determination. The complex crystallised with a mixture of coordinated solvent which was also confirmed by microanalysis and ^{1}H NMR spectroscopy (thf:thp ~ 1:1). The compound was found to loose coordinated solvent even at ambient pressure. DRIFT ($\tilde{\nu}$): 3077 (w), 3051 (w), 2979 (w), 2941 (w), 2860 (w), 1899 (vw), 1585 (s), 1572 (s), 1534 (w), 1480 (s), 1441 (w), 1389 (vw), 1327 (w), 1283 (m), 1192 (w), 1171 (m), 1146 (w), 1077 (w),1033 (s), 980 (m), 966 (w), 866 (m), 849 (m), 810 (m), 801 (m), 749 (s), 741 (s), 695 (vs), 639 (vs), 569 (m), 524 (vs), 469 (s), 442 (m) cm^{-1}. Elemental analysis (%) calculated for mixted thf/thp complex (1:1) $C_{83}H_{110}Sm_4O_6$ (1805.23 g/mol): C 55.22, H 6.14, N 0.00; found: C 53.88, H 5.64, N 0.03.

[Eu(CH$_2$Ph)$_2$]$_n$ (1-Eu). Following the procedure described for **1-Yb** using EuI$_2$(thf)$_2$ (401 mg, 0.73 mmol) dissolved in 5 mL of thf and [K(CH$_2$Ph)]$_n$ (190 mg, 1.46 mmol) dissolved in 3 mL of thf afforded **1-Eu** as an orange solid (238 mg, 0.71 mmol, 98%). Elemental analyses showed slight deviations, most likely due to traces of residual iodide which could not be separated in the workup procedure. DRIFT ($\tilde{\nu}$): 3052 (w), 2976 (w), 2876 (w), 2565 (vw), 1916 (w), 1782 (vw), 1688 (vw), 1584 (vs), 1570 (vs), 1534 (w), 1479 (vs), 1444 (w), 1326 (w), 1283 (s), 1176 (m), 1148 (w), 1034 (w), 980 (m), 848 (w), 801 (w), 741 (m), 700 (m), 654 (m), 533 (s), 512 (m), 484 (m), 463 (w) cm^{-1}. Elemental analysis (%) calculated for C$_{14}$H$_{14}$Eu (334.23 g/mol): C 50.31, H 4.21, N 0.00; found: C 49.12, H 4.58, N 0.03.

[(thf)$_2$Eu$_4$(CH$_2$Ph)$_8$] (1-Eu^{thf}). A solution of **1-Eu** (50 mg) in thf (1 mL) was carefully layered with *n*-hexane (1 mL) and stored at –35 °C for one week which led to the formation of dark orange crystals along with a dark orange oil. These crystals were suitable for X-ray structure determination but immediate loss of coordinated thf solvent even at ambient pressure together with difficult separation from the oily phase hampered determination of yield and further analysis. Elemental analysis (%) calculated for C$_{64}$H$_{72}$Eu$_4$O$_2$ (1484.13 g/mol): C 51.90, H 4.90, N 0.00; found: C 49.88, H 4.54, N 0.38.

[(thf)Yb(NDipp)]$_4$ (2-Yb). To a solution of [Yb(CH$_2$Ph)$_2$]$_n$ (**1-Yb**, 178 mg, 0.50 mmol) in thp (1 mL) was added a solution of H$_2$NDipp (88 mg, 0.50 mmol) in thp (2 mL). The resulting deep red solution was stirred at ambient temperature for 60 h and filtered. The solvent was removed at reduced pressure, leaving a dark red oily residue which was dissolved in a small amount of thf. Again, the solvent was removed at reduced pressure and the residue was dissolved in a mixture of thf and *n*-hexane (1:1). Storage of the solution at –35 °C for 7 days afforded the product as dark red crystalline solid which was separated from the mother liquor and dried at reduced pressure. Yield: 122 mg, 0.07 mmol, 58%. Crystals suitable for X-ray structure determination were obtained from a saturated thf solution at –35 °C after several weeks. ^{1}H NMR (400 MHz, [D$_8$]thf, 26 °C): δ 6.68 (d, 2H, $^3J_{HH}$ 7.4 Hz, *m*-Ar*H*), 5.91 (t, 1H, $^3J_{HH}$ 7.3 Hz, *p*-Ar*H*), 3.62 (m, 4H, OC*H*$_2$ thf), 3.28 (m, 2H, *i*Pr-C*H*), 1.78 (m, 4H, C*H*$_2$ thf), 1.18 (d, 12H, $^3J_{HH}$ 6.6 Hz, *i*Pr-C*H*$_3$) ppm. ^{13}C{^{1}H} NMR (101 MHz, [D$_8$]thf, 26 °C): δ 161.9 (*ipso*-Ar*C*), 135.4 (*o*-Ar*C*), 123.9 (*m*-Ar*C*), 107.5 (*p*-Ar*C*), 68.4 (O*C*H$_2$ thf), 30.2 (*i*Pr-*C*H), 26.5 (*C*H$_2$ thf), 24.4 (*i*Pr-*C*H$_3$) ppm. DRIFT ($\tilde{\nu}$): 3069 (vw), 3025 (vw), 2952 (s), 2870 (w), 1577 (m), 1529 (vw), 1456 (w), 1421 (w), 1386 (vs), 1368 (s), 1349 (m), 1289 (m), 1234 (vs), 1131 (m), 1031 (m), 918 (w), 877 (s), 839 (m), 790 (vw), 740 (s), 732 (s), 681 (w), 619 (w),

543 (w), 454 (m), 446 (m) cm^{-1}. Elemental analysis (%) calculated for $C_{64}H_{100}N_4O_4Yb_4$ (1681.74 g/mol): C 45.71, H 5.99, N 3.33; found: C 45.56, H 5.68, N 3.36.

[(thf)Eu(NDipp)]$_4$ (2-Eu). To a solution of $[Eu(CH_2Ph)_2]_n$ (**1-Eu**, 65 mg, 0.19 mmol) in thp (1 mL) was added a solution of H_2NDipp (35 mg, 0.19 mmol) in thp (1 mL). The resulting orange solution was stirred at ambient temperature for 60 h and filtered. The solvent was removed at reduced pressure, leaving a dark orange oily residue which was dissolved in a small amount of thf. Again, the solvent was removed at reduced pressure and the residue was dissolved in a mixture of thf and *n*-hexane (1:1). Storage of the solution at –35 °C for 7 days afforded the product as orange crystalline solid which was separated from the mother liquor and dried at reduced pressure. Yield: 48 mg, 0.03 mmol, 62%. Crystals suitable for X-ray structure determination were obtained from a saturated thf/*n*-hexane (1:1) solution at –35 °C. DRIFT ($\tilde{\nu}$): 3064 (vw), 3021 (w), 2954 (m), 2868 (w), 1577 (m), 1523 (w), 1456 (w), 1384 (vs), 1365 (s), 1298 (s), 1233 (vs), 1130 (m), 1035 (w), 918 (vw), 877 (w), 834 (w), 732 (w), 679 (vw), 539 (vw), 440 (w) cm^{-1}. Elemental analysis (%) calculated for $C_{64}H_{100}N_4O_4Eu_4$ (1597.38 g/mol): C 48.12, H 6.31, N 3.51; found: C 48.01, H 6.29, N 3.60.

Crystallography

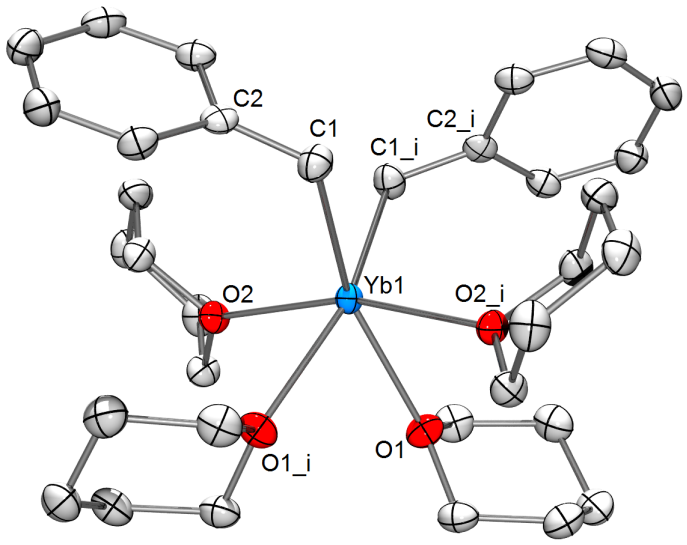

Figure S1. Solid-state structure of **1-Yb^{thp}**. Hydrogen atoms are omitted for clarity. Atomic displacement ellipsoids were set at 50% probability. Selected bond lengths [Å] and angles [°]: Yb1–C1 2.617(3), Yb1–C2 3.495, Yb1–O1 2.502(2), Yb1–O2 2.468(2); C1–Yb1–O1 96.07(9), C1–Yb1–O1_i 158.80(6), C1–Yb1–O2 81.55(6), C1–Yb1–O2_i 109.58(6), C1–Yb1–C1_i 93.02(13), O1–Yb1–O1_i 82.10(10), O1–Yb1–O2 90.72(6), O1–Yb1–O2_i 77.37(6), O2–Yb1–O2_i 164.28(8), Yb1–C1–C2 115.89(14).

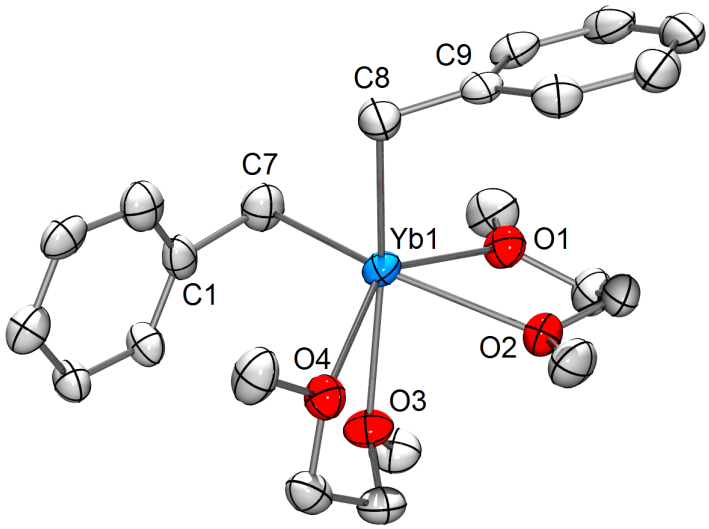

Figure S2. Solid-state structure of **1-Yb^{dme}**. Hydrogen atoms and the disorder in one of the phenyl groups are omitted for clarity. Atomic displacement ellipsoids were set at 50% probability. Selected bond lengths [Å] and angles [°]: Yb1–C7 2.585(2), Yb1–C8 2.572(2), Yb1–C1 2.943(9), Yb1–C9 3.1722(19), Yb1–O1 2.470(2), Yb1–O2 2.4941(15), Yb1–O3 2.4917(16), Yb1–O4 2.493(2); C7–Yb1–O2 155.27(6), C8–Yb1–O3 163.37(6), O1–Yb1–O4 138.84(6), C7–Yb1–C8 97.09(8), O1–Yb1–O2 65.97(5), O3–Yb1–O4 65.68(5), Yb1–C7–C1 90.8(4), Yb1–C8–C9 100.70(11).

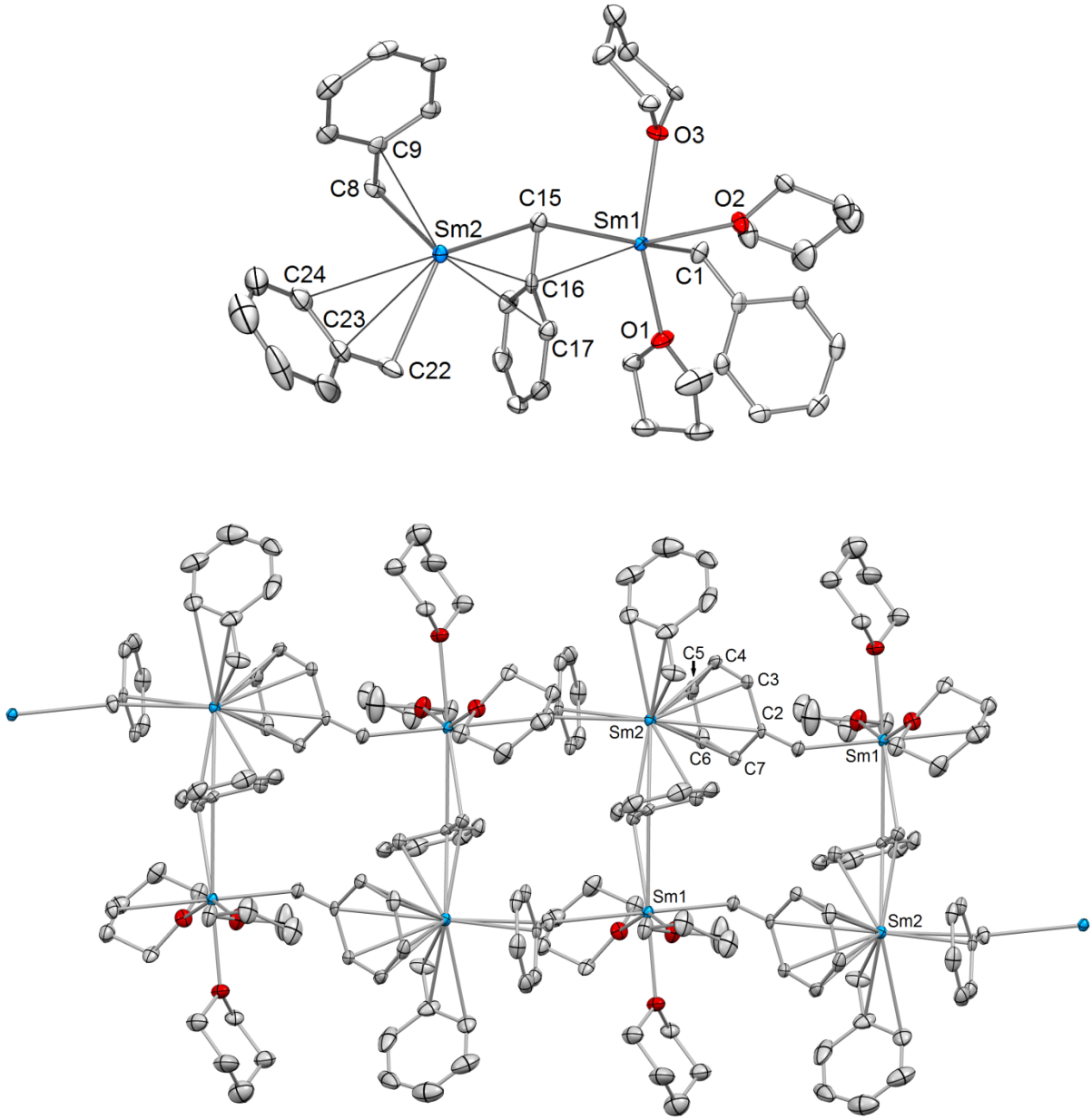

Figure S3. Solid-state structure of **1-Sm^{do}** (top: asymmetric unit, bottom: polymeric arrangement). Hydrogen atoms, the disorder of two of the donor molecules (partial disorder of thf/thp), and the disorder of one benzyl group (C22) are omitted for clarity. Atomic displacement ellipsoids were set at 50% probability. Selected bond lengths [Å] and angles [°]: Sm1–C1 2.782(4), Sm1–C16 2.920(3), Sm1–C15 2.836(3), Sm2–C8 2.901(4), Sm2–C9 2.916(4), Sm2–C15 2.830(3), Sm2–C16 2.920(3), Sm2–C17 3.101, Sm2–C22 2.704(6), Sm2–C23 3.032(4), Sm2–C24 3.149, Sm2–C2 3.243, Sm2–C3 3.021(4), Sm2–C4 2.892(4), Sm2–C5 2.877(4), Sm2–C6 2.973(3), Sm2–C7 3.121; Sm1–C15–Sm2 155.3(1), C1–Sm1–C15 83.5(1), O2–Sm1–C15 81.2(1), O1–Sm1–O3 78.78(8), C8–Sm2–C15 81.9(1), C8–Sm2–C22 102.1(2).

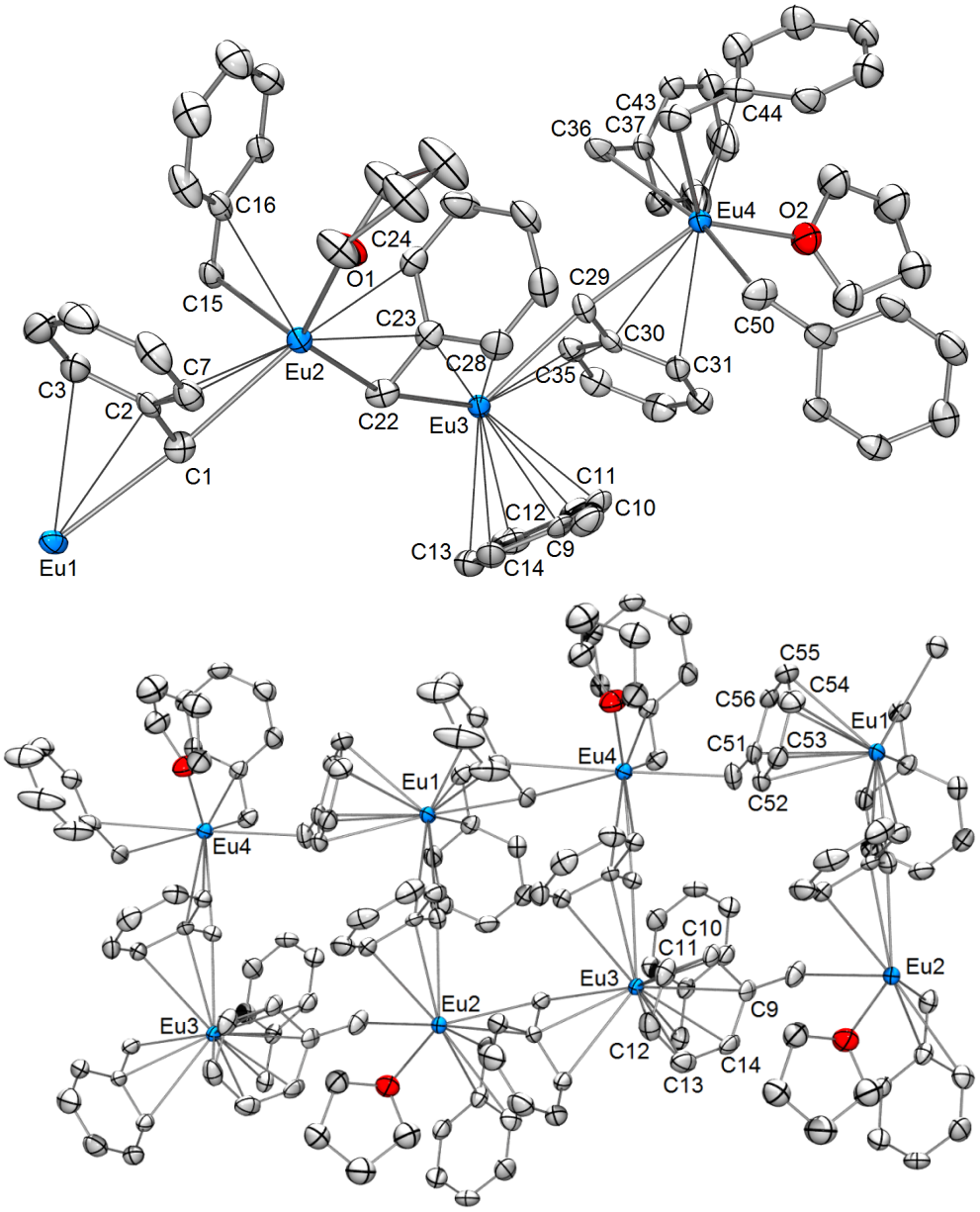

Figure S4. Solid-state structure of **1-Eu^{thf}** (top: asymmetric unit, bottom: polymer arrangement). Hydrogen atoms and the disorder in both thf molecules are omitted for clarity. Atomic displacement ellipsoids were set at 50% probability. Selected bond lengths [Å]: Eu1–C1 2.761(7), Eu1–C2 3.089(6), Eu1–C3 3.205, Eu1–C36 2.818(7), Eu1–C37 2.908(7), Eu1–C38 3.118(7), Eu1–C43 2.753(8), Eu1–C44 2.921(7), Eu1–C45 3.343, Eu1–C51 3.182(7), Eu1–C52 2.971(7), Eu1–C53 2.884(7), Eu1–C54 2.912(8), Eu1–C55 2.997(8), Eu1–C56 3.119(7), Eu2–C1 2.842(7), Eu2–C2 2.992(6), Eu2–C7 3.005(7), Eu2–C8 2.834(7), Eu2–C15 2.888(7), Eu2–C16 3.171(7), Eu2–C22 2.812(7), Eu2–C23 2.949(7), Eu2–C24 3.297,Eu2–O1 2.530(5), Eu3–C9 3.167, Eu3–C10 2.959(7), Eu3–C11 2.891(8), Eu3–C12 2.899(8), Eu3–C13 3.009(8), Eu3–C14 3.098(7), Eu3–C15 2.826(7), Eu3–C16 2.920(6), Eu3–C17 3.083(7), Eu3–C22 2.761(8), Eu3–C23 2.942(7), Eu3–C29 2.767(7), Eu3–C28 3.338, Eu3–C30 3.083(6), Eu3–C35 3.184, Eu4–C29 2.828(7), Eu4–C30 2.985(6), Eu4–C31 2.993(7), Eu4–C36 2.875(7), Eu4–C37 3.251(8), Eu4–C43 2.811(8), Eu4–C44 2.952(7), Eu4–C49 3.380, Eu4–C50 2.837(7), Eu4–O2 2.512(6).

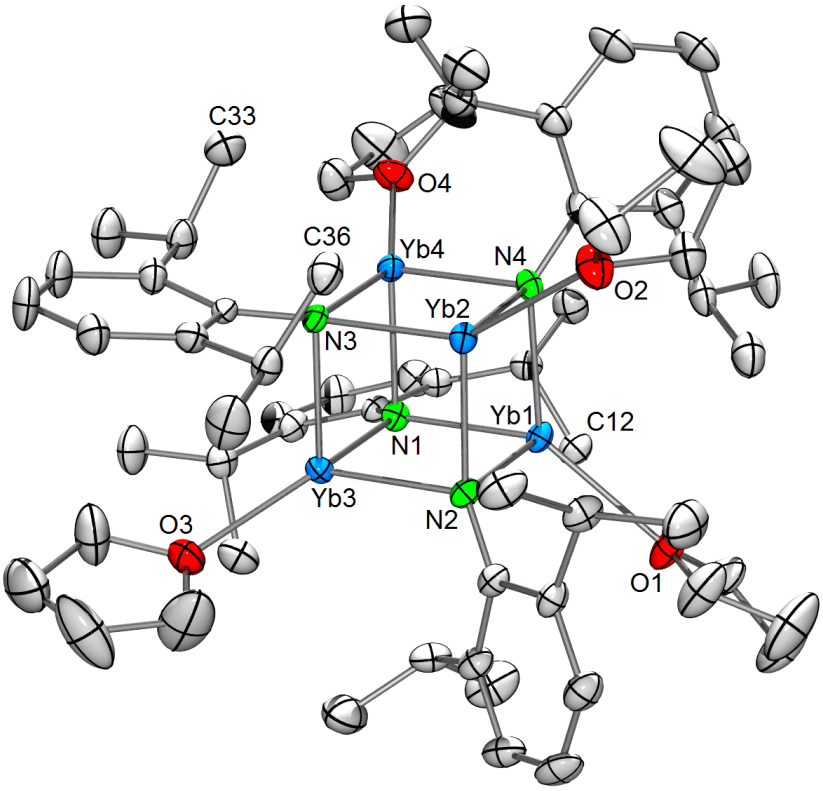

Figure S5. Solid-state structure of **2-Yb**. Hydrogen atoms and lattice solvent (two molecules of disordered thf) are omitted for clarity. Atomic displacement ellipsoids were set at 50% probability. For selected bond lengths and angles see Table S1 below.

Table S1. Selected bond lengths and angles for complex **2-Yb**.

bond lengths [Å]		**bond angles [°]**	
Yb1–N1	2.430(5)	Yb4–N1–Yb3	91.4(2)
Yb1–N2	2.361(5)	Yb4–N1–Yb1	90.2(2)
Yb1–N4	2.412(4)	Yb3–N1–Yb1	91.0(2)
Yb2–N2	2.407(4)	Yb1–N2–Yb3	93.0(2)
Yb2–N3	2.416(5)	Yb1–N2–Yb2	90.7(2)
Yb2–N4	2.357(5)	Yb3–N2–Yb2	91.3(2)
Yb3–N1	2.383(5)	Yb3–N3–Yb4	91.4(2)
Yb3–N2	2.370(5)	Yb3–N3–Yb2	91.6(2)
Yb3–N3	2.352(4)	Yb4–N3–Yb2	91.6(2)
Yb4–N1	2.374(4)	Yb2–N4–Yb4	94.2(2)
Yb4–N3	2.405(4)	Yb2–N4–Yb1	90.7(2)
Yb4–N4	2.360(5)	Yb4–N4–Yb1	91.0(2)
Yb1–O1	2.557(4)	N2–Yb1–N4	89.1(2)
Yb2–O2	2.568(4)	N2–Yb1–N1	87.6(2)
Yb3–O3	2.444(4)	N4–Yb1–N1	88.1(2)

bond lengths [Å]		bond angles [°]	
Yb4–O4	2.451(4)	N4–Yb2–N2	89.3(2)
Yb1–C12	2.954(6)	N4–Yb2–N3	87.0(2)
Yb2–C36	2.945(6)	N2–Yb2–N3	87.4(2)
Yb4–C33	3.090(7)	N3–Yb3–N2	89.7(2)
		N3–Yb3–N1	89.1(2)
		N2–Yb3–N1	88.5(2)
		N4–Yb4–N1	90.6(2)
		N4–Yb4–N3	87.2(2)
		N1–Yb4–N3	88.0(2)

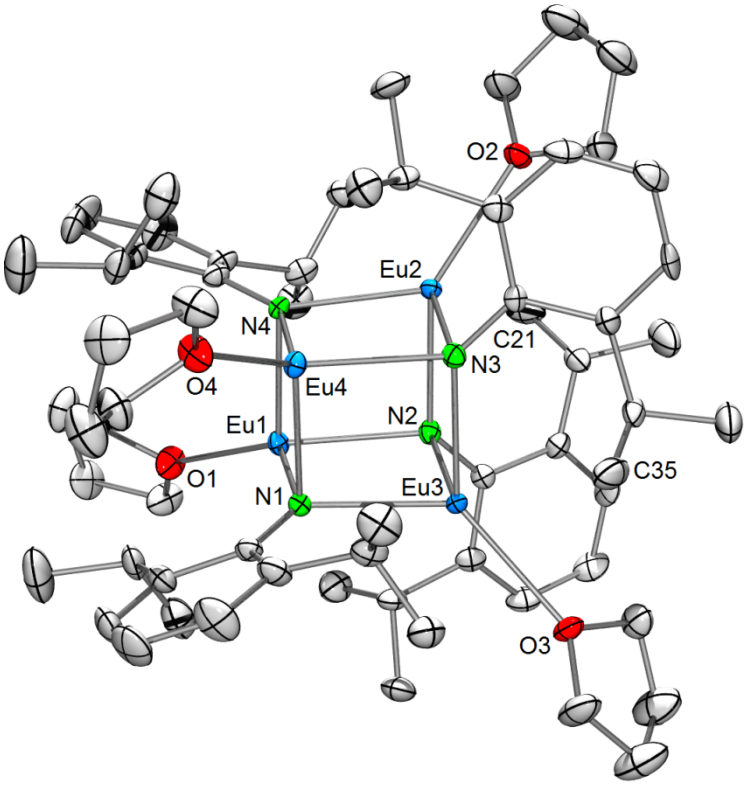

Figure S6. Solid-state structure of **2-Eu**. Hydrogen atoms are omitted for clarity. Atomic displacement ellipsoids were set at 50% probability. For selected bond lengths and angles see Table S2 below.

Table S2. Selected bond lengths and angles for complex **2-Eu**.

bond lengths [Å]		**bond angles [°]**	
Eu1–N1	2.509(4)	Eu4–N1–Eu3	93.7(1)
Eu1–N2	2.514(4)	Eu4–N1–Eu1	94.6(2)
Eu1–N4	2.482(4)	Eu3–N1–Eu1	93.3(1)
Eu2–N2	2.516(5)	Eu1–N2–Eu3	93.9(1)
Eu2–N3	2.474(4)	Eu3–N2–Eu2	95.7(1)
Eu2–N4	2.504(4)	Eu1–N2–Eu2	92.6(1)
Eu3–N1	2.501(4)	Eu2–N3–Eu4	93.8(1)
Eu3–N2	2.473(4)	Eu2–N3–Eu3	95.6(2)
Eu3–N3	2.519(5)	Eu4–N3–Eu3	92.5(1)
Eu4–N1	2.480(4)	Eu1–N4–Eu2	93.6(1)
Eu4–N3	2.515(4)	Eu1–N4–Eu4	94.5(2)
Eu4–N4	2.512(4)	Eu2–N4–Eu4	93.1(1)
Eu1–O1	2.656(4)	N4–Eu1–N1	85.5(1)
Eu2–O2	2.669(4)	N4–Eu1–N2	86.9(1)
Eu3–O3	2.673(4)	N1–Eu1–N2	85.7(1)
Eu4–O4	2.654(4)	N3–Eu2–N4	86.9(1)
Eu2–C21	3.252(6)	N3–Eu2–N2	84.4(2)
Eu3–C35	3.247(6)	N4–Eu2–N2	86.4(1)
		N2–Eu3–N1	86.8(1)
		N2–Eu3–N3	84.4(2)
		N1–Eu3–N3	86.4(1)
		N1–Eu4–N4	85.4(1)
		N1–Eu4–N3	86.9(1)
		N4–Eu4–N3	85.8(1)

Table S3. Crystallographic data for compounds **1-Yb^{thp}**, **1-Yb^{dme}**, and **1-Sm^{do}**

	1-Yb^{thp}	**1-Yb^{dme}**	**1-Sm^{do}**
formula	$C_{34}H_{54}O_4Yb$	$C_{22}H_{34}O_4Yb$	$C_{84}H_{112}O_6Sm_4$
CCDC	1852184	1852188	1852183
M_r [g mol^{-1}]	699.81	535.53	1819.13
color	orange/rod	red/plate	black/rod
crystal dimensions [mm]	0.205 x 0.074 x 0.068	0.305 x 0.300 x 0.146	0.091 x 0.089 x 0.053
cryst syst	monoclinic	monoclinic	triclinic
space group	*C*2/c	$P2_1/c$	$P\bar{1}$
a [Å]	9.536(8)	13.172(11)	12.252(6)
b [Å]	16.441(16)	12.265(5)	12.490(8)
c [Å]	20.897(16)	14.497(7)	12.826(5)
α [°]	90	90	84.442(17)
β [°]	96.14(2)	90.35(4)	77.873(10)
γ [°]	90	90	80.73(6)
V [Å^3]	3257(5)	2342(3)	1890(2)
Z	4	4	1
T [K]	150(2)	180(2)	100(2)
ρ_{calcd} [g cm^{-3}]	1.427	1.519	1.598
μ [mm^{-1}]	2.905	4.014	3.113
F (000)	1440	1072	912
θ range [°]	1.960/28.282	2.175/28.282	1.627/28.282
unique reflns	4038	5800	9361
observed reflns (I>2σ)	3775	5289	7639
R1/*w*R2 (I>2σ)[a]	0.0210/0.0495	0.0156/0.0382	0.0265/0.0541
R1/*w*R2 (all data)[a]	0.0235/0.0502	0.0187/0.0397	0.0391/0.0593
GOF[a]	1.043	1.040	1.041

[a] $R1 = \Sigma(||F_0|-|F_c||)/\Sigma|F_0|$, $F_0 > 4\sigma(F_0)$. $wR2 = \{\Sigma[w(F_0^2-F_c^2)^2/\Sigma[w(F_0^2)^2]\}^{1/2}$.

Table S4. Crystallographic data for compounds **1-Eu^{thf}**, **2-Yb**, and **2-Eu**

	1-Eu^{thf}	**2-Yb**	**2-Eu**
formula	$C_{32}H_{36}Eu_2O$	$C_{64}H_{100}N_4O_4Yb_4 \cdot 2\ C_4H_8O$	$C_{64}H_{100}Eu_4N_4O_4$
CCDC	1852186	1852185	1852187
M_r [g mol^{-1}]	740.53	1824.83	1597.31
color	orange/plate	brown/block	red/rod
crystal dimensions [mm]	0.191 x 0.127 x 0.124	0.466 x 0.458 x 0.258	0.355 x 0.124 x 0.063
cryst syst	triclinic	monoclinic	monoclinic
space group	$P\bar{1}$	Pc	$P2_1$
a [Å]	12.4889(13)	13.2322(8)	12.8719(2)
b [Å]	14.9634(16)	16.2283(10)	24.3507(4)
c [Å]	15.0111(16)	17.9608(11)	13.4375(2)
α [°]	94.734(3)	90	90
β [°]	94.590(3)	111.614(2)	118.6090(10)
γ [°]	90.111(3)	90	90
V [Å^3]	2786.6(5)	3585.6(4)	3697.61(10)
Z	4	2	2
T [K]	170(2)	140(2)	100(2)
ρ_{calcd} [g cm^{-3}]	1.765	1.690	1.435
μ [mm^{-1}]	4.482	5.219	3.386
F (000)	1448	1806	1592
θ range [°]	1.366/27.103	1.255/29.578	1.726/27.484
unique reflns	12272	20088	16968
observed reflns (I>2σ)	8622	19608	16082
R1/*w*R2 (I>2σ)[a]	0.0432/0.1027	0.0237/0.0573	0.0218/0.0467
R1/*w*R2 (all data)[a]	0.0712/0.1231	0.0246/0.0577	0.0247/0.0473
GOF[a]	1.063	1.025	1.048

[a] $R1 = \Sigma(||F_0|-|F_c||)/\Sigma|F_0|$, $F_0 > 4\sigma(F_0)$. $wR2 = \{\Sigma[w(F_0^2-F_c^2)^2/\Sigma[w(F_0^2)^2]\}^{1/2}$.

X-ray Crystallography and Crystal Structure Determinations. Crystals of **1-Yb^{thp}**, **1-Yb^{dme}**, **1-Sm^{do}**, **1-Eu^{thf}**, **2-Yb**, and **2-Eu** were grown by standard techniques from saturated solutions using thp (**1-Yb^{thp}**), a mixture of dme and toluene (**1-Yb^{dme}**), a mixture of thf, thp and *n*-hexane (**1-Sm^{do}**), a mixture of thf and *n*-hexane (**1-Eu^{thf}**, **2-Eu**) or thf (**2-Yb**). Suitable crystals for X-ray structure analyses were selected in a glovebox and coated with Parabar 10312 (previously known as Paratone N, Hampton Research) and fixed on a nylon loop/glass fiber.

X-ray data for above mentioned compounds were collected on a Bruker APEX II DUO (**2-Eu**) or a APEX III DUO (all remaining; instruments equipped with an IμS microfocus sealed tube and QUAZAR optics for MoKα (λ = 0.71073 Å) and CuKα (λ = 1.54184 Å) radiation. The data collection strategy was determined using COSMO[4] employing ω- and Φ-scans (APEX II) or ω-scans (APEX III). Raw data were processed using APEX[5] and SAINT,[6] corrections for absorption effects were applied using SADABS.[7] The structures were solved by direct methods and refined against all data by full-matrix least-squares methods on F^2 using SHELXTL[8] and SHELXLE.[9] All graphics were produced employing ORTEP-3[10] and POV-Ray.[11] Further details of the refinement and crystallographic data are listed in Table S3 and S4, and in the CIF files. CCDC depositions 1852183-1852188 contain all the supplementary crystallographic data for this paper. These data can be obtained free of charge from The Cambridge Crystallographic Data Centre via www.ccdc.cam.ac.uk/structures/.

NMR spectroscopy

Notes on NMR spectroscopic characterisations.

Due to the nearly identical shifts of resonances in compounds **1-Yb**, **1-Yb^{thp}** and **1-Yb^{dme}** in [D_8]thf it is likely that in all cases the thf solvate is formed in solution. Due to the paramagnetic nature of Sm(II) and Eu(II) any conclusive interpretation of the recorded NMR spectra was not possible. In general solvent peaks are marked with an asterisk (*).

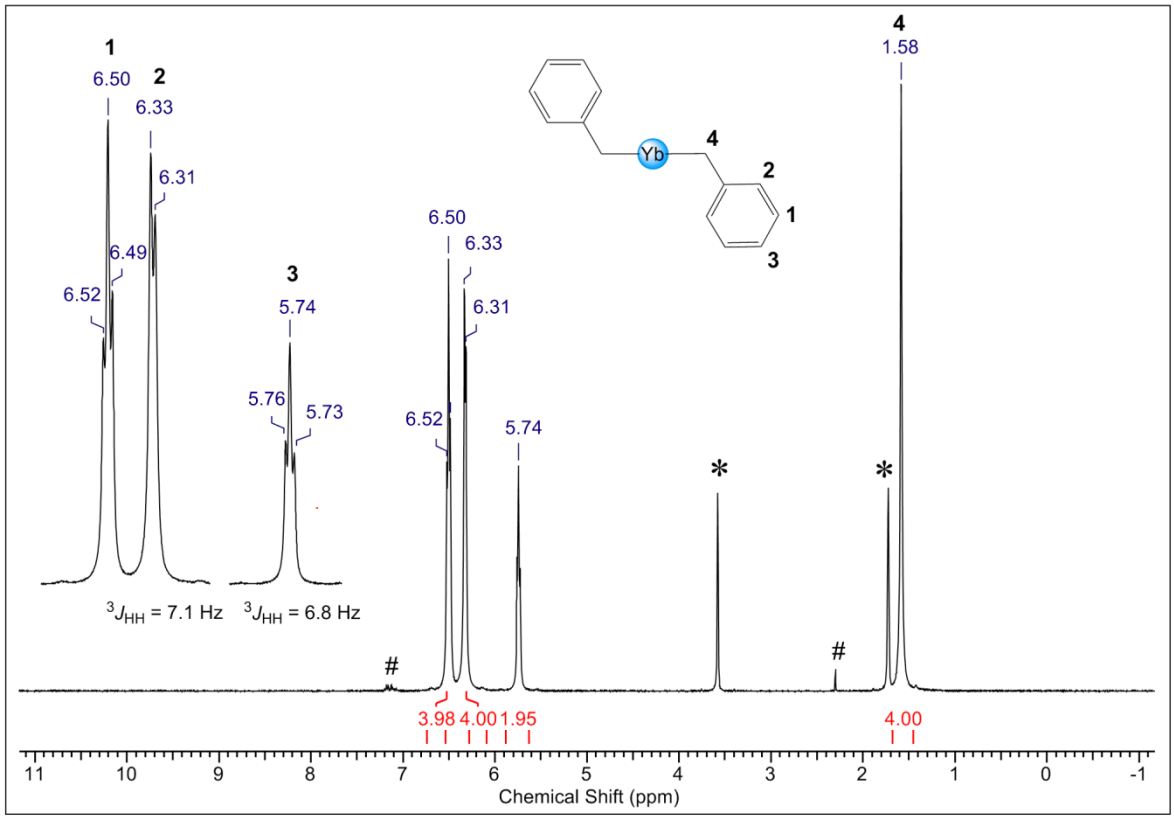

Figure S7. ^{1}H NMR spectrum (400 MHz, [D$_8$]thf, 26 °C) of [Yb(CH$_2$Ph)$_2$]$_n$ (**1-Yb**) (# denotes traces of toluene).

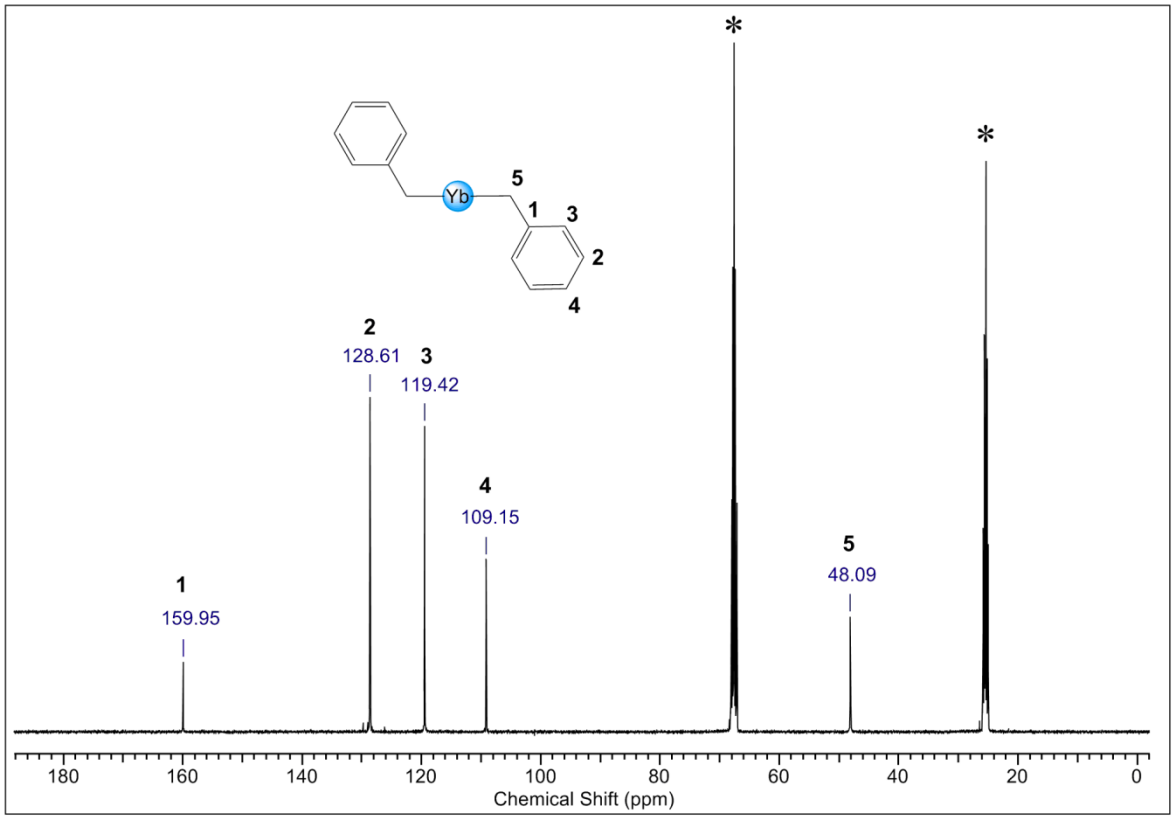

Figure S8. ^{13}C{^{1}H} NMR spectrum (101 MHz, [D$_8$]thf, 26 °C) of [Yb(CH$_2$Ph)$_2$]$_n$ (**1-Yb**).

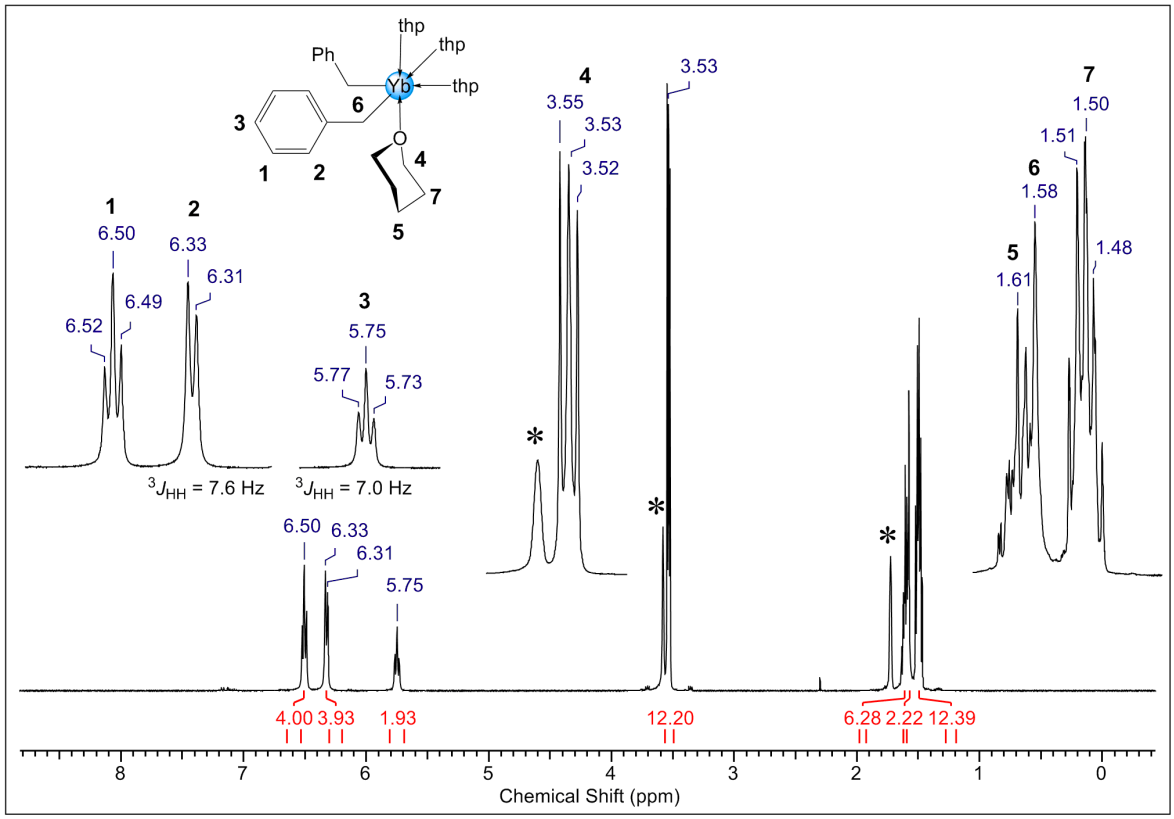

Figure S9. ^{1}H NMR spectrum (400 MHz, [D$_8$]thf, 26 °C) of [(thp)$_4$Yb(CH$_2$Ph)$_2$] (**1-Yb^{thp}**).

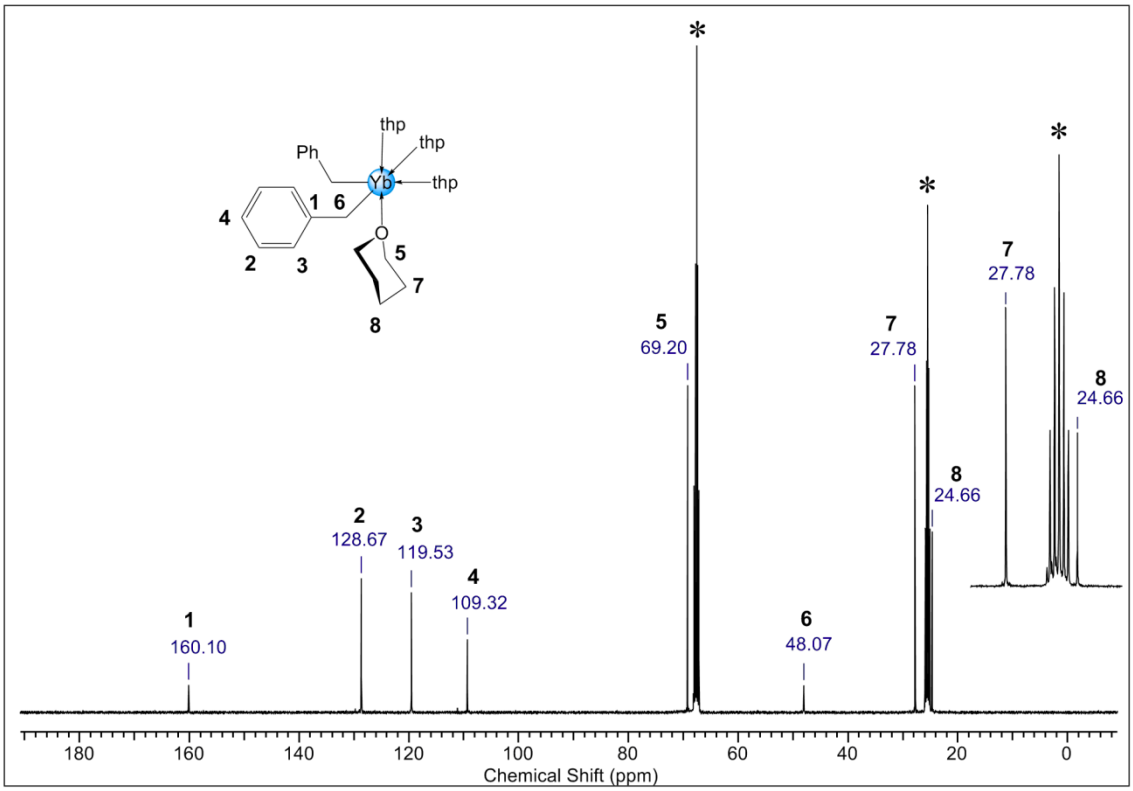

Figure S10. ^{13}C{^{1}H} NMR spectrum (101 MHz) of [(thp)$_4$Yb(CH$_2$Ph)$_2$] (**1-Yb^{thp}**) in [D$_8$]thf at 26 °C.

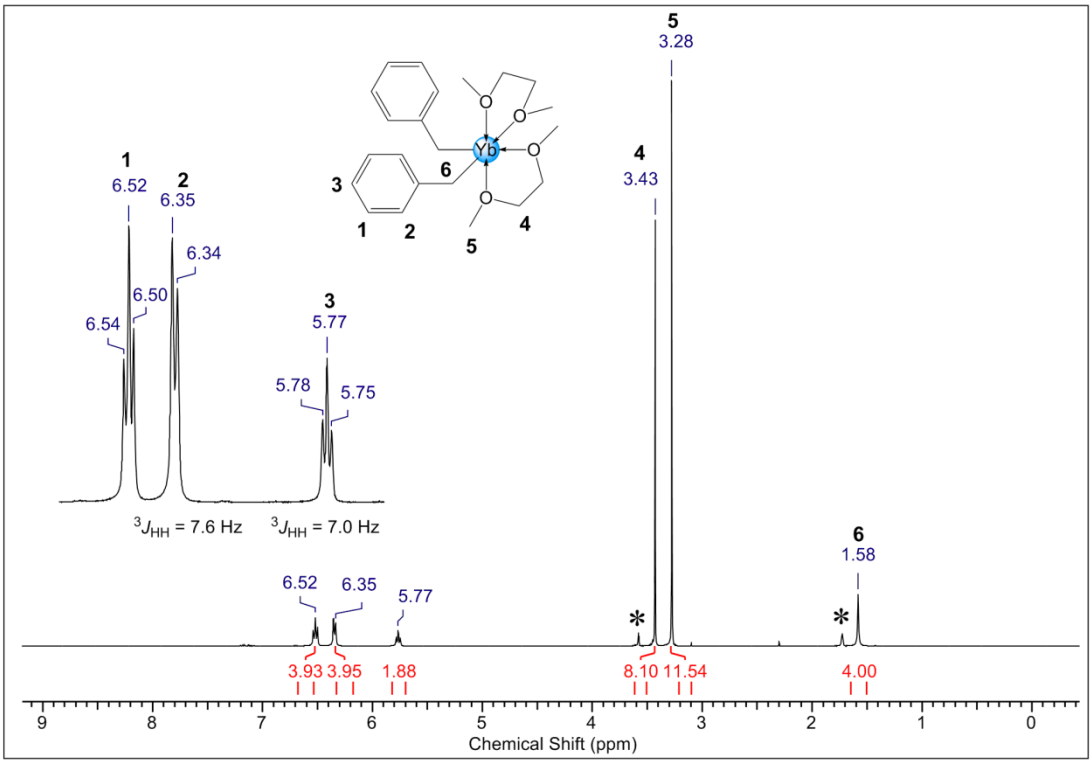

Figure S11. ^{1}H NMR spectrum (400 MHz, [D$_8$]thf, 26 °C) of [(dme)$_2$Yb(CH$_2$Ph)$_2$] (**1-Yb^{dme}**).

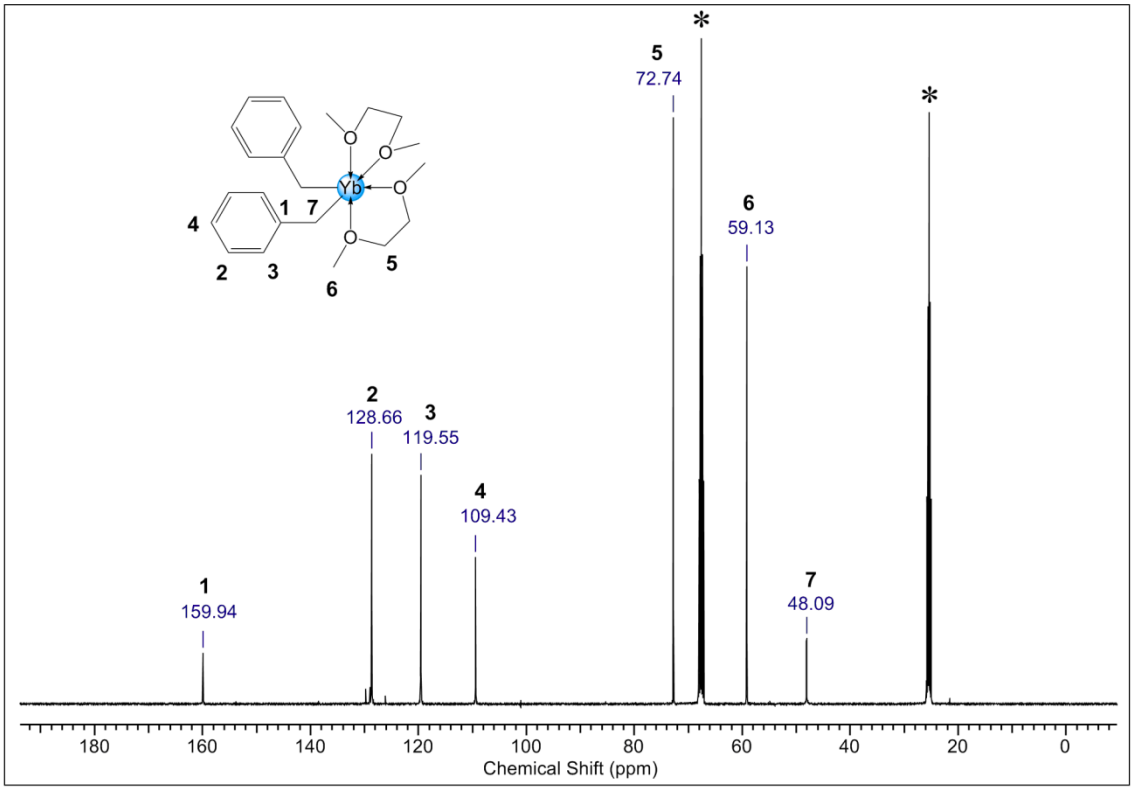

Figure S12. ^{13}C{^{1}H} NMR spectrum (101 MHz, [D$_8$]thf, 26 °C) of [(dme)$_2$Yb(CH$_2$Ph)$_2$] (**1-Yb^{dme}**).

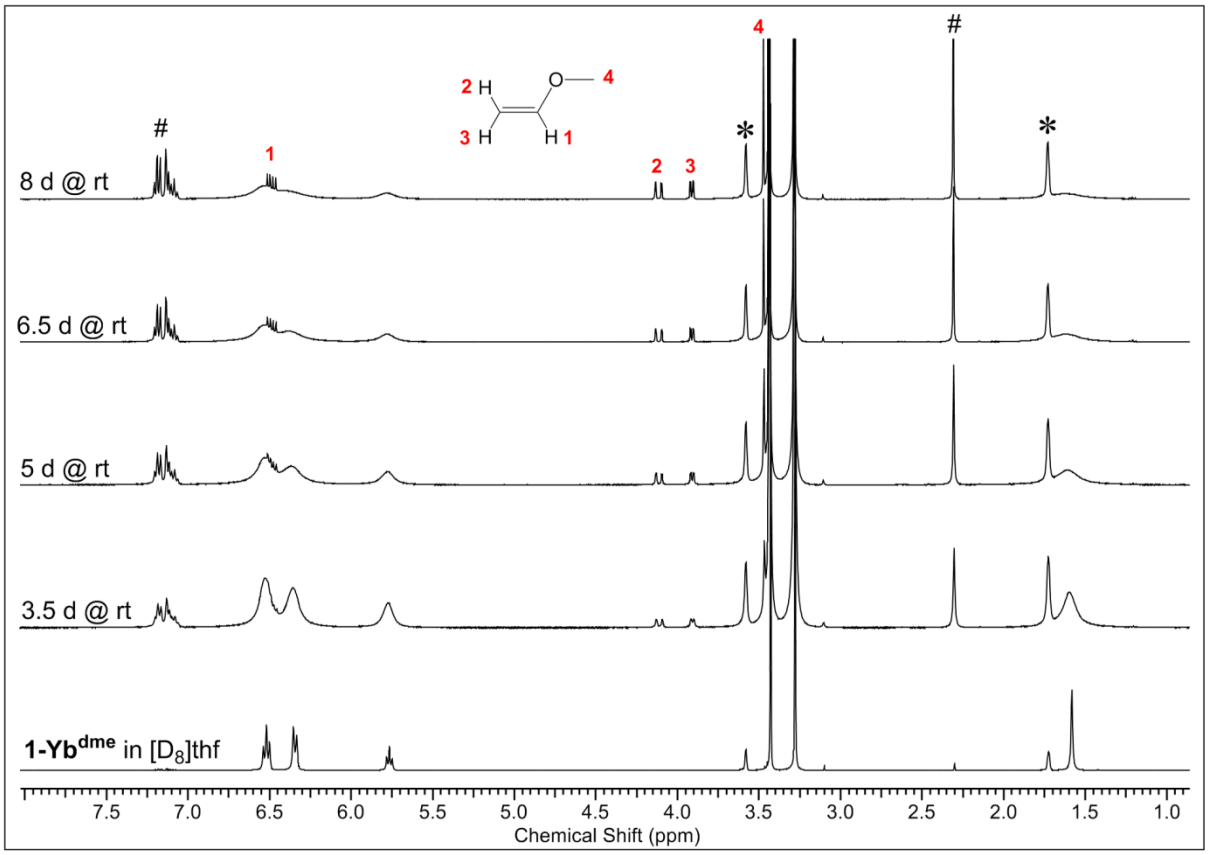

Figure S13. ^{1}H NMR spectra (400 MHz, [D_8]thf, 26 °C) of [(dme)$_2$Yb(CH_2Ph)$_2$] (**1-Yb^{dme}**) over time. Decomposition was observed accompanied by formation of toluene (#), methyl vinyl ether (base induced ether cleavage of dme), and by formation of an insoluble precipitate (most likely a Yb–OMe species).

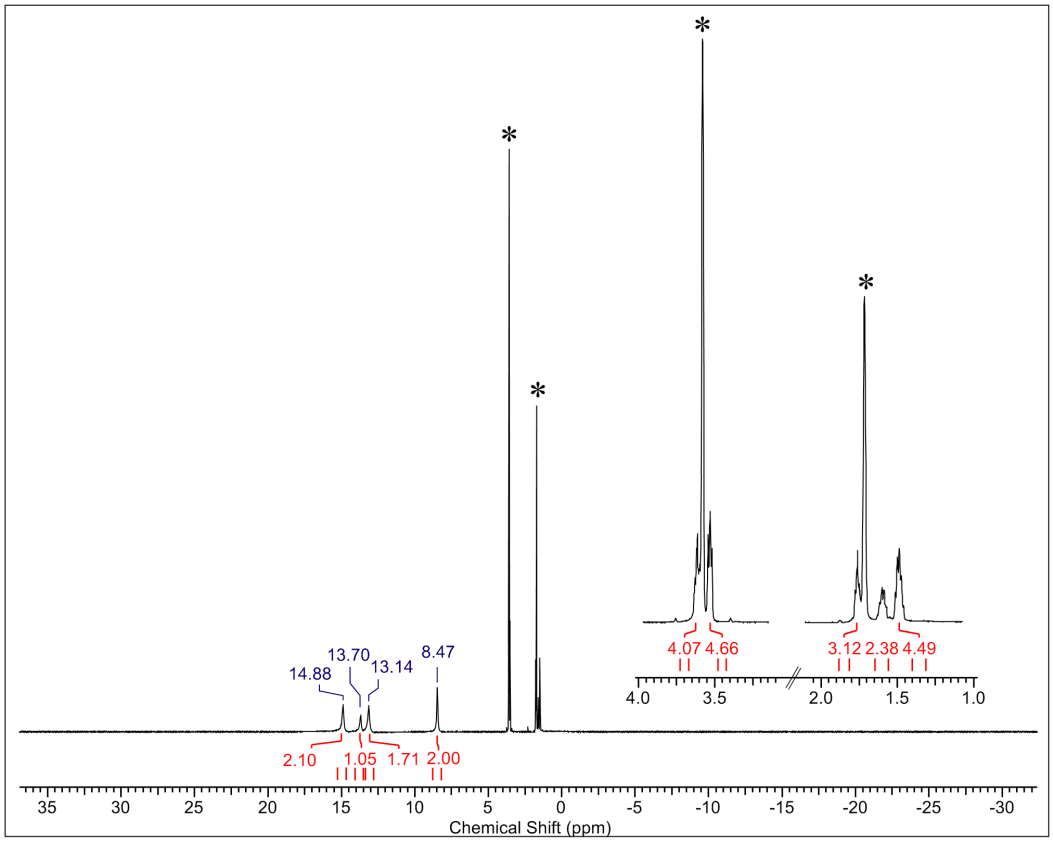

Figure S14. ^{1}H NMR spectrum (400 MHz, [D_8]thf, 26 °C) of [$(do)_3Sm_2(CH_2Ph)_4$] (**1-Sm^{do}**). Replacement of coordinated donor solvents (mixture of thf and thp) allowed for an estimation of the thf/thp ratio as ~1.0:1.1.

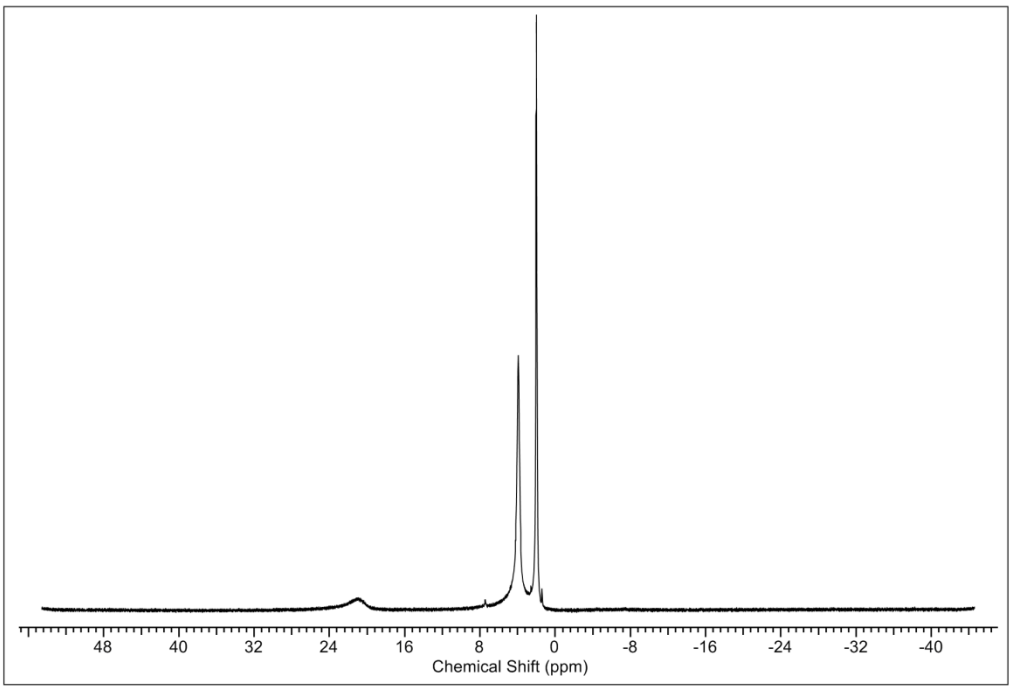

Figure S15. ^{1}H NMR spectrum (400 MHz, [D_8]thf, 26 °C) of [$(thf)_2Eu_4(CH_2Ph)_8$] (**1-Eu^{thf}**).

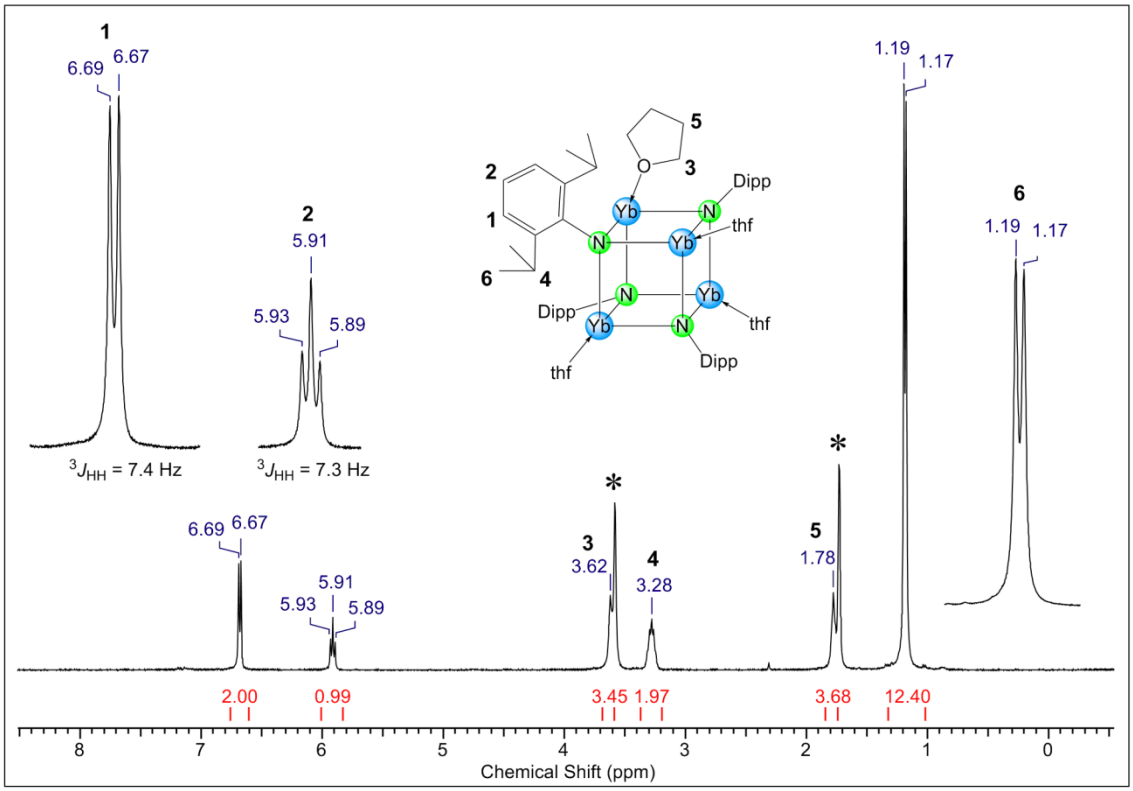

Figure S16. ^{1}H NMR spectrum (400 MHz, [D$_8$]thf, 26 °C) of [(thf)Yb(NDipp)]$_4$ (**2-Yb**).

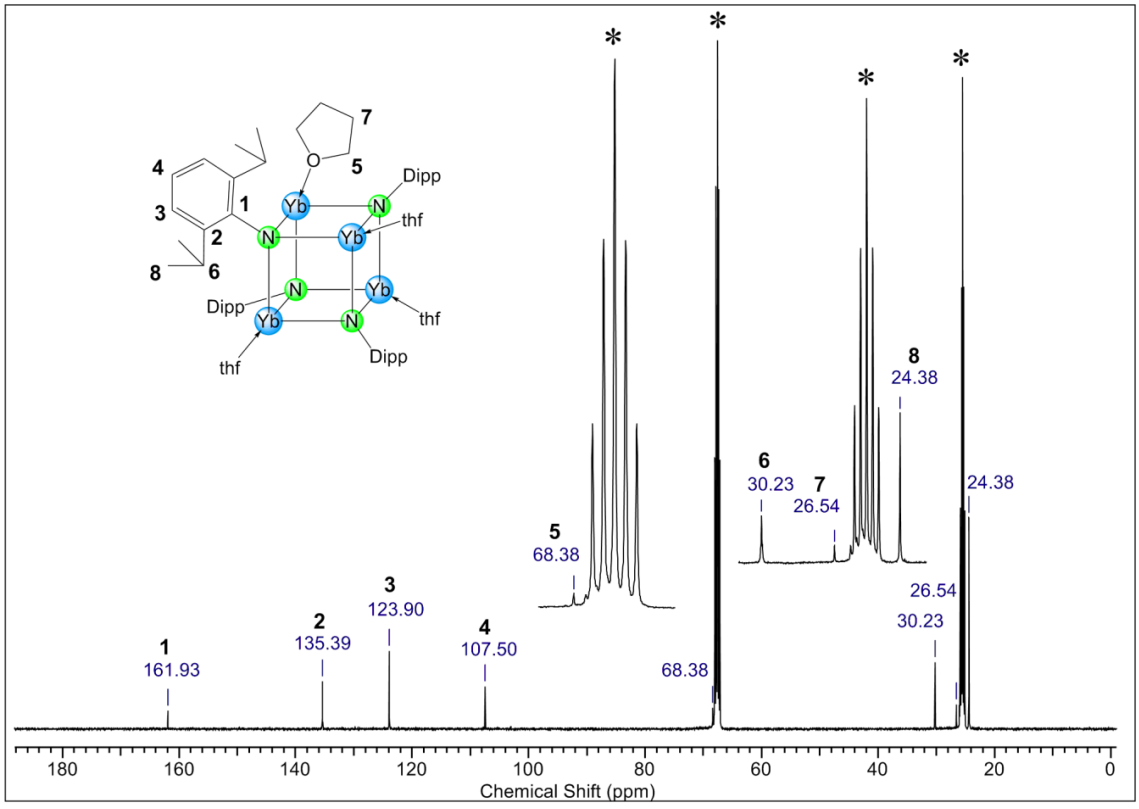

Figure S17. ^{13}C{^{1}H} NMR spectrum (101 MHz, [D$_8$]thf, 26 °C) of [(thf)Yb(NDipp)]$_4$ (**2-Yb**).

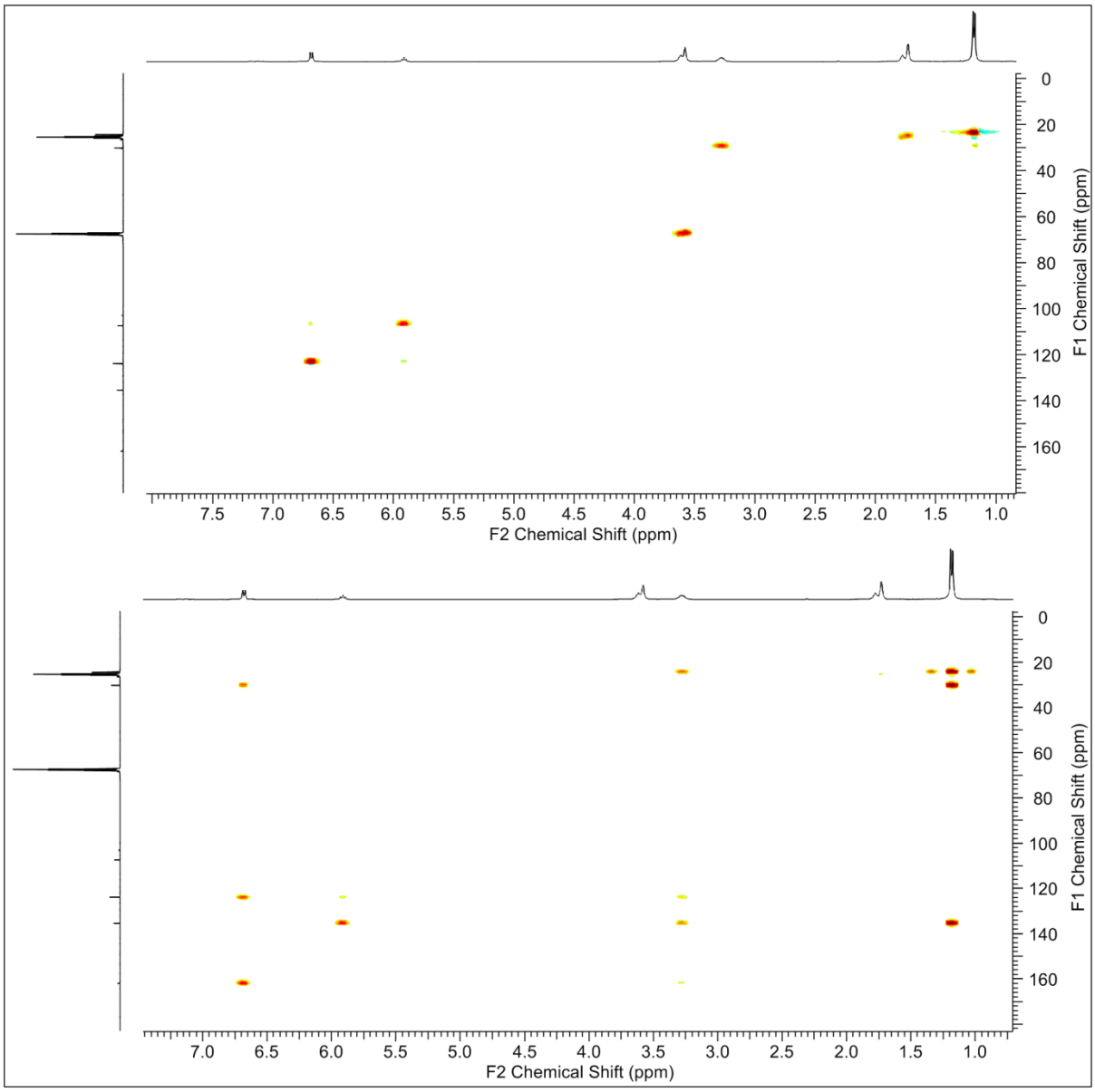

Figure S18. $^{1}H^{13}C$-HSQC NMR spectrum (top, 400/101 MHz, [D_8]thf, 26 °C) and $^{1}H^{13}C$-HMBC NMR spectrum (bottom, 400/101 MHz, [D_8]thf, 26 °C) of [(thf)Yb(NDipp)]$_4$ (**2-Yb**).

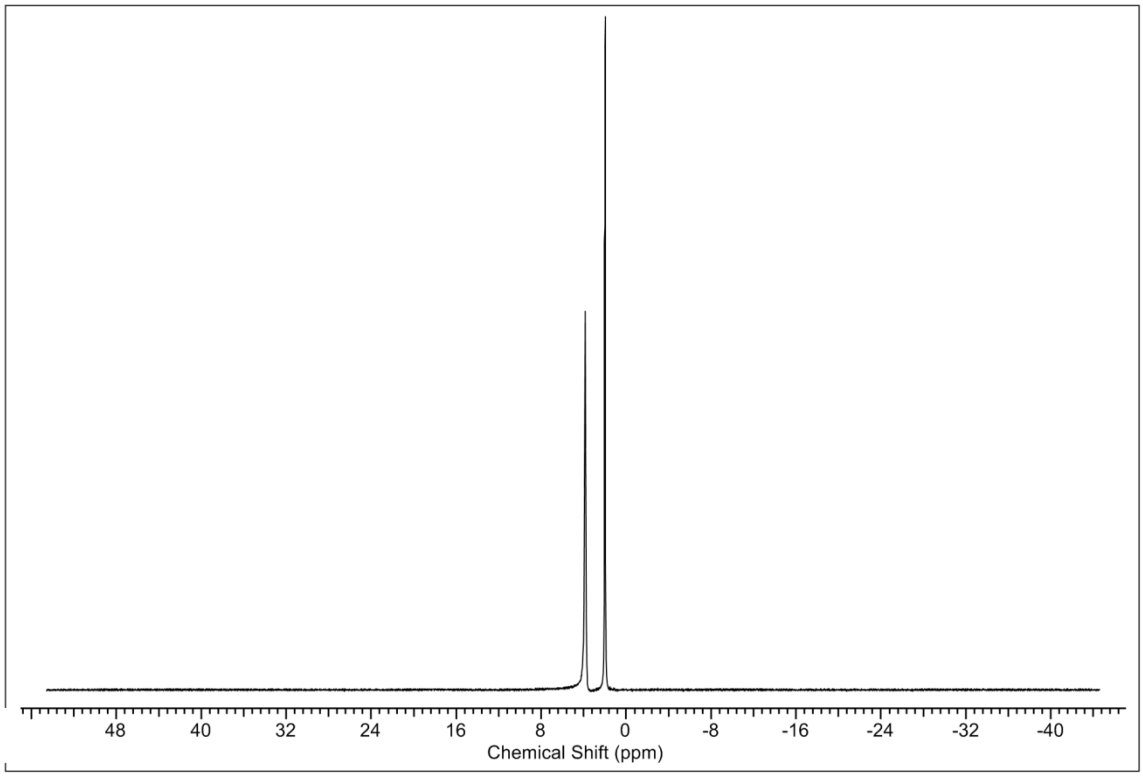

Figure S19. ^{1}H NMR spectrum (400 MHz, [D_8]thf, 26 °C) of [(thf)Eu(NDipp)]$_4$ (**2-Eu**).

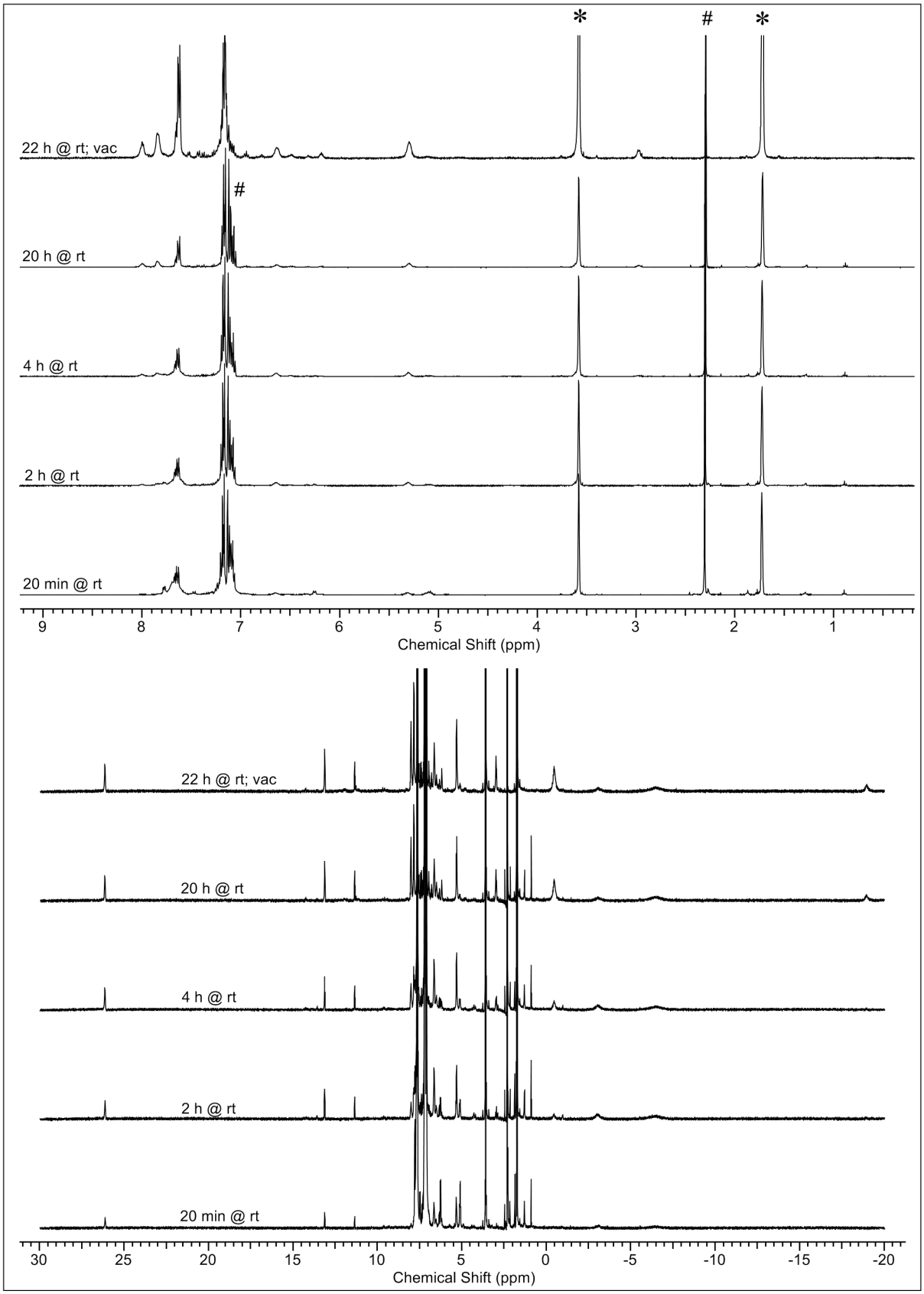

Figure S20. ^{1}H NMR (400 MHz, [D_8]thf, 26 °C) monitored reaction of $[Yb(CH_2Ph)_2]_n$ (**1-Yb**) with one equivalent of H_2NSiPh_3 showing paramagnetic Yb(III) side products (# denotes toluene; vac = solvents were removed and residue was redissolved in [D_8]thf).

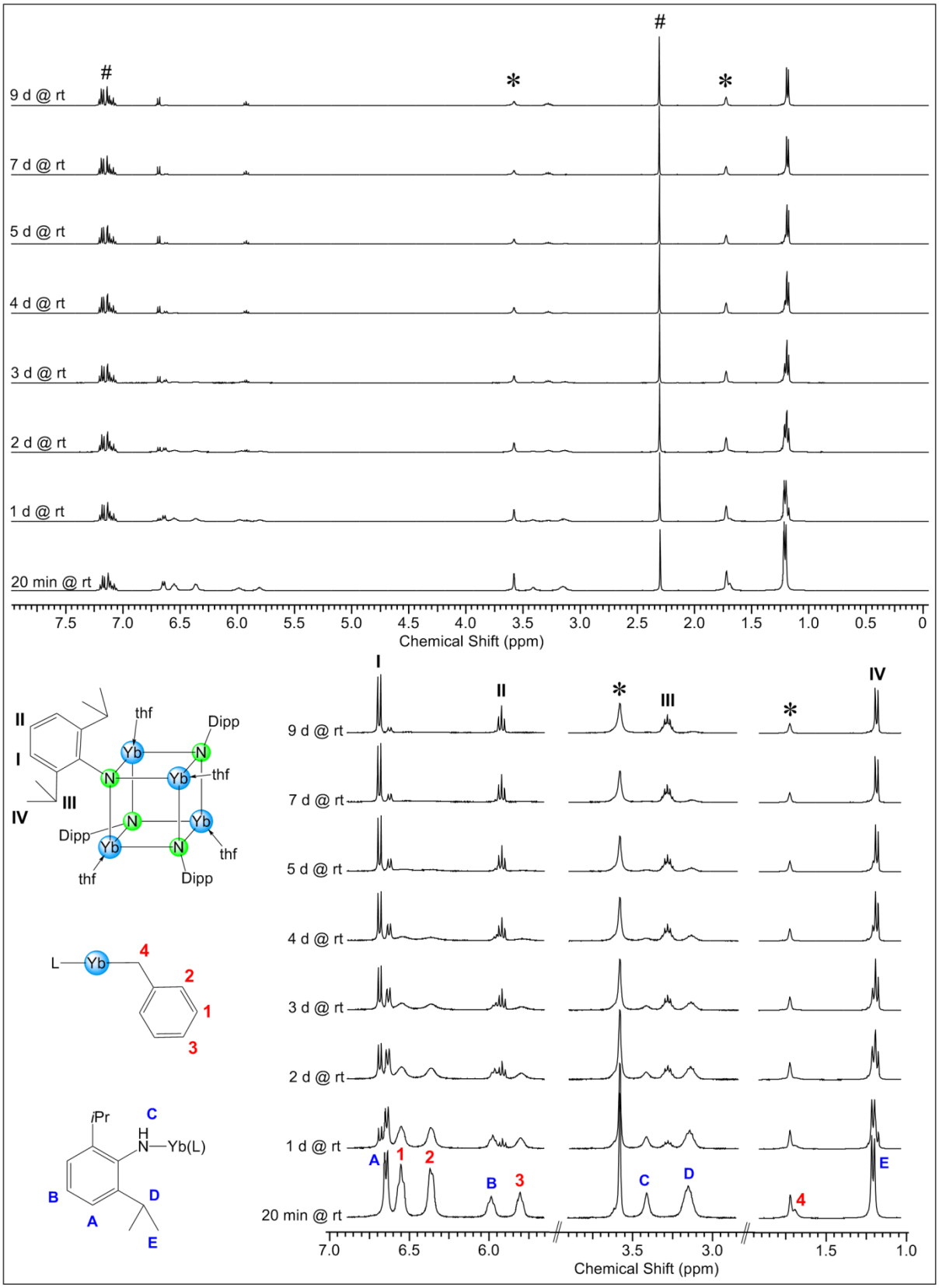

Figure S21. Reaction of $[Yb(CH_2Ph)_2]_n$ (**1-Yb**) with one equivalent of H_2NDipp monitored by ^1H NMR spectroscopy (400 MHz, $[D_8]$thf, 26 °C) (# denotes toluene).

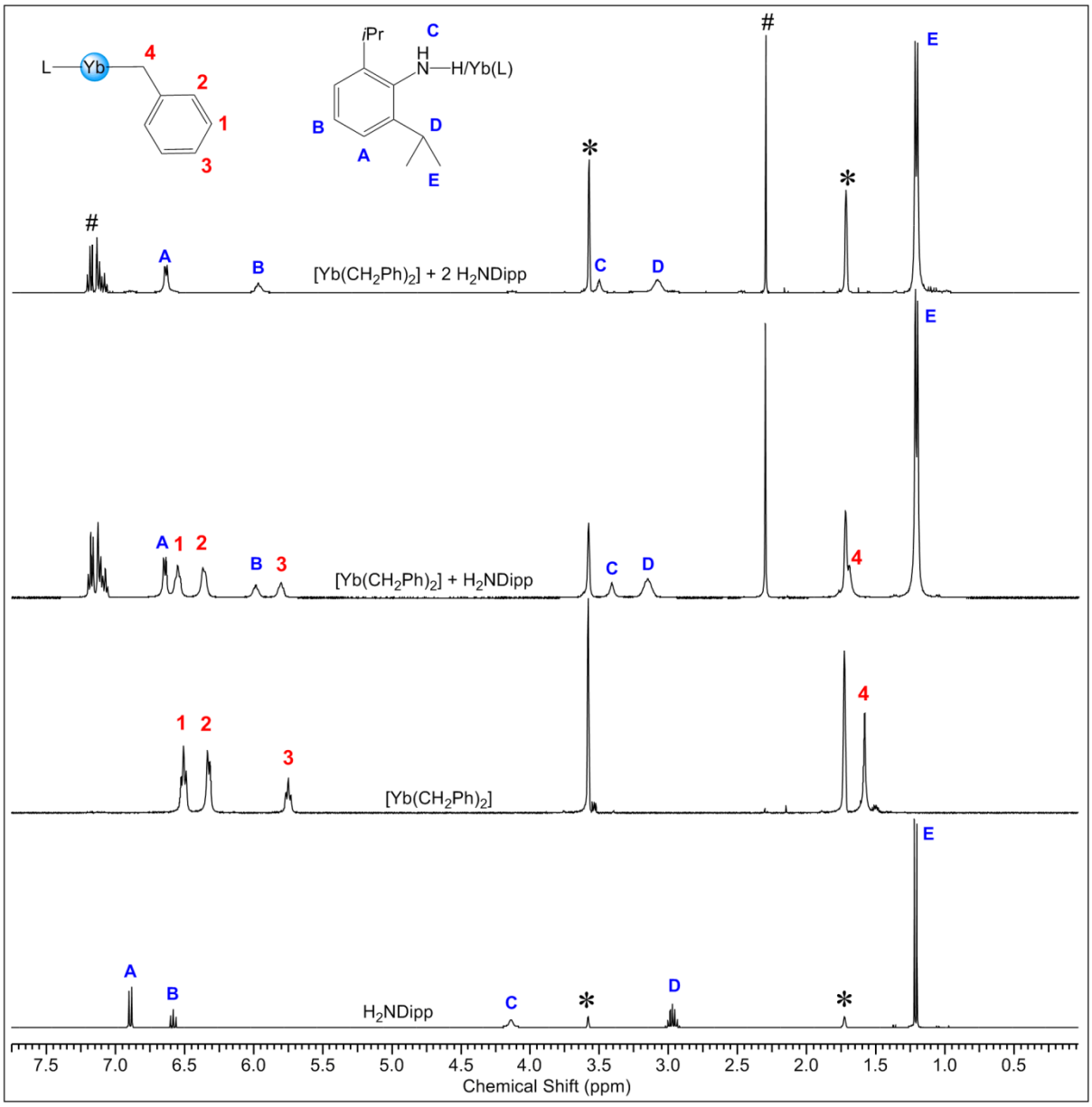

Figure S22. Comparison of the ^{1}H NMR spectra (400 MHz, [D$_8$]thf, 26 °C) of H_2NDipp and $[Yb(CH_2Ph)_2]_n$ (**1-Yb**) to *in situ* ^{1}H NMR spectra of the reaction of $[Yb(CH_2Ph)_2]_n$ with one and two equivalents of H_2NDipp. Despite a slight shift found for some resonances of the intermediate species of the imide reaction (20 min @ rt) compared to **1-Yb** and homoleptic $[(thf)_xYb(NHDipp)_2]$, the nature of this intermediate remained unclear (# denotes toluene).

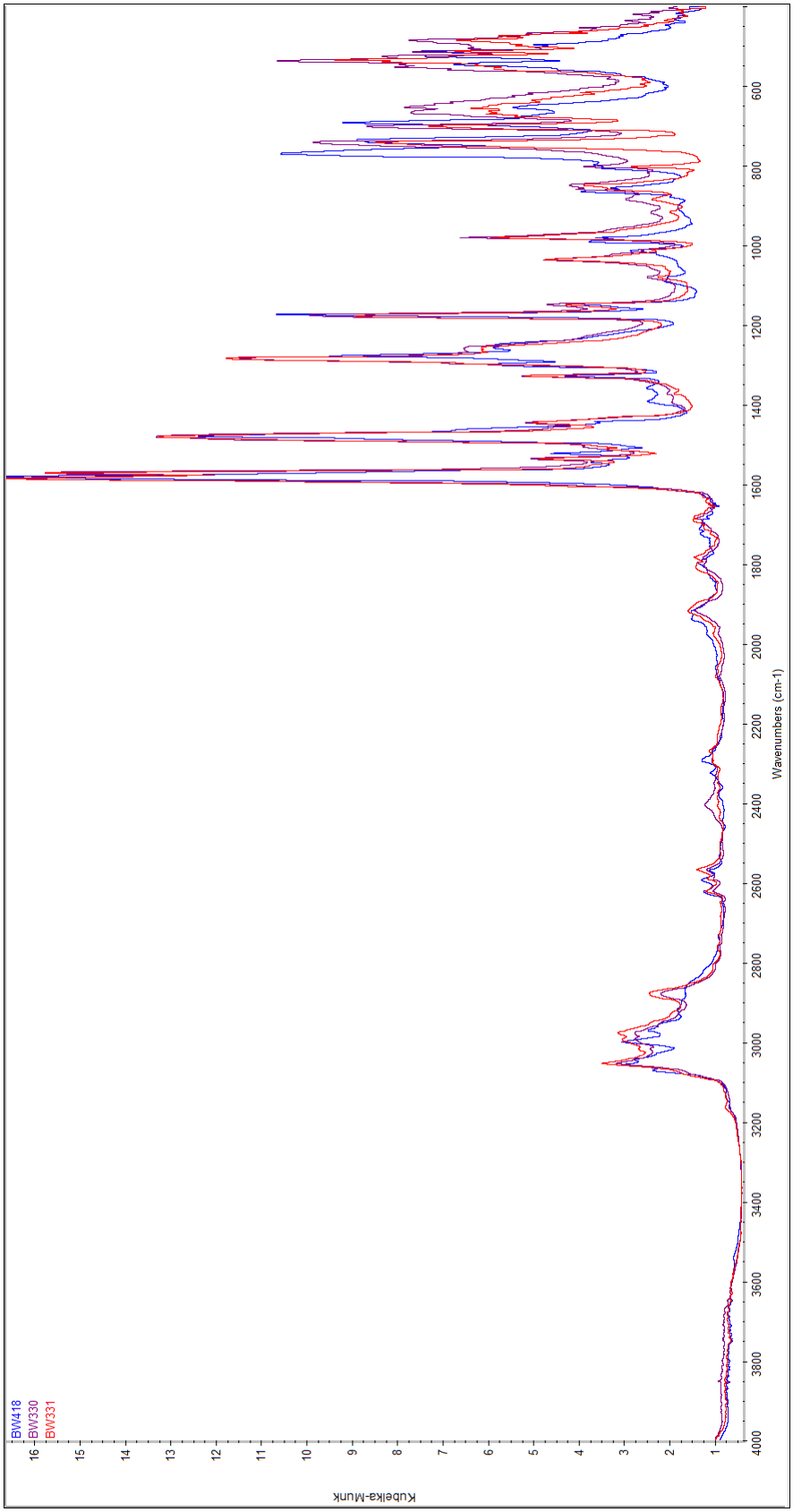

Figure S23. DRIFT spectra of dibenzyl compounds $[Ln(CH_2Ph)_2]_n$ (**1-Ln**; Ln = Sm, purple; Ln = Eu, red; Ln = Yb. blue).

References

1 P. Girard, J. L. Namy and H. B. Kagan, *J. Am. Chem. Soc.* 1980, **102**, 2693−2698.

2 P. J. Bailey, R. A. Coxall, C. M. Dick, S. Fabre, L. C. Henderson, C. Herber, S. T. Liddle, D. Loroño-González, A. Parkin and S. Parsons, *Chem. Eur. J.* 2003, **9**, 4820–4828.

3 S. M. I. Al-Rafia, P. A. Lummis, M. J. Ferguson, R. McDonald and E. Rivard, *Inorg. Chem.* 2010, **49**, 9709–9717.

4 COSMO, v. 1.61; Bruker AXS Inc.: Madison, WI, 2012.

5 a) APEX 2 v. 2012.10_0, Bruker AXS Inc., Madison, WI, 2012; b) APEX 3, v. 2016.5-0; Bruker AXS Inc., Madison, WI, 2016.

6 a) SAINT, v. 8.34A; Bruker AXS Inc., Madison, WI, 2013; b) SAINT, v. 8.37A; Bruker AXS Inc., Madison, WI, 2015.

7 a) a) SADABS v. 2012/1, G.M. Sheldrick, AXS Inc., Madison, WI, 2012; b) SADABS: L. Krause, R. Herbst-Irmer, G. M. Sheldrick and D. Stalke, *J. Appl. Crystallogr.* 2015, **48**, 3.

8 SHELXTL v. 2012.10_2, G.M. Sheldrick, Bruker AXS Inc., Madison, WI, 2012.

9 SHELXLE: C. B. Hübschle, G. M. Sheldrick and B. Dittrich, *J. Appl. Crystallogr.* 2011, **44**, 1281-1284.

10 ORTEP: a) L. J. Farrugia, *J. Appl. Crystallogr.* 1997, **30**, 565-566; L. J. Farrugia, *J. Appl. Crystallogr.* 2012, **45**, 849-854.

11 POV-Ray v. 3.6; Persistence of Vision Pty. Ltd.: Williamstown, Victoria, Australia, 2004. http://www.povray.org/ .